38th International Electric Vehicle Symposium and Exhibition (EVS38)
Göteborg, Sweden, June 15-18, 2025

Challenges in the realiable detection of lithium plating using dynamic electrochemical impedance spectroscopy

Raphael Urban, Mathieu Seyfritz-Combo, Christian Peter, Cristina Grosu, Markus Lienkamp
Technical University of Munich (TUM), School of Engineering & Design,
Department of Mobility Systems Engineering, Institute of Automotive Technology,
raphael.urban@tum.de

Executive Summary

Extreme fast-charging will be a key requirement for the widespread adoption of battery electric vehicles. However, in those extreme conditions, the probability of lithium metal deposition as a critical ageing mechanism is increased and needs to be reliably detected to avoid accelerated battery degradation during a fast-charging process. Dynamic electrochemical impedance spectroscopy is a non-destructive testing method that provides insights into the internal degradation processes during the charging procedure without current interruption. To exploit the full potential of the measurement, a real-time target current specification based on the impedance data is necessary to derive an impedance-based charging algorithm. Therefore, lithium plating must be reliably detected under various operating conditions. Many publications in the literature have proven the effectiveness of the method, but the derived data quality and the parameters used in the post-processing step have a major influence on the result, which needs to be critically discussed. In order to evaluate the influence of different initial SOCs and various parameters in the post-processing step of the data, a series of experiments were conducted. It could be shown that unsuitable parameters during the smoothing process can lead to a false positive detection of the lithium-plating onset and therefore, would lead to a higher charging time in an impedance-based fast-charging process.
Keywords: Batteries, AC & DC Charging technology, Smart charging, Battery Management System, Electric Vehicles

1 Introduction

Lithium-ion batteries (LIB) are widely used in battery electric vehicles (BEV) due to their high energy density, high charge/discharge current capability, and low self-discharge rate [1]. Despite their advantages, range anxiety and high charging times compared to the refueling of conventional internal combustion engine (ICE) vehicles remain among the main disadvantages of the widespread adoption of BEV [2]. The United States Department of Energy (DOE) proposed a target charging time of below $15\,\mathrm{min}$ [3]. However, reduced charging times accelerate the degradation of the LIBs, causing a decrease in capacity and an increase in internal resistance. Lithium plating is considered to be a crucial ageing mechanism during fast-charging that causes rapid capacity fade and the growth of dendrites, which can lead to a short circuit and thus to a thermal runaway [4]. The metallic deposition of lithium is thermodynamically possible when the anode potential drops below $0\,\mathrm{V}$ vs. $\mathrm{Li/Li^+}$ [5]. High states of charge [6], high charging rates [7] and low temperatures [8, 9] promote the onset of lithium plating. The reliable detection of the metallic deposition is of utmost importance for the development of a health-aware fast-charging protocol.

Electrochemical impedance spectroscopy (EIS) is a non-destructive technique, which allows the identification and separation of different electrochemical processes inside the LIB, that proceed at differing rates [10]. In galvanostatic mode, the battery impedance is obtained by applying a sinusoidal current excitation at a specific frequency and measuring the corresponding voltage response of the cell [11]. When EIS is performed at different frequencies, an impedance spectrum is created, which can be viewed in a Nyquist plot (Figure 1). By superimposing the alternating current (AC) excitation with the direct current (DC) used for charging, dynamic electrochemical impedance spectroscopy (DEIS) can be derived, which allows the analysis of the battery impedance during the charging process without interruption.
According to Uhlmann et al. [12], the ionic current inside the battery during a charging event with lithium plating can be divided into two components: (i) the intercalation current, carrying lithium ions into the graphite, and (ii) the plating current, which contributes to lithium metal deposition and therefore, reduces the flow of lithium ions available for intercalation. The plating reaction introduces an additional impedance $\mathrm{Z}_{Plating}$ in parallel to the charge transfer impedance $\mathrm{Z}_{CT(N)}$ of the anode [13]. This is expected to lead to a reduction of the semi-circle in the Nyquist-plot, representing $\mathrm{Z}_{CT(N)}$ + $\mathrm{Z}_{CT(P)}$ + Z_{SEI} + Z_{CEI} [13, 14]. $\mathrm{Z}_{CT(P)}$ describes the charge transfer impedance at the cathode, Z_{SEI} the impedance of the solid electrolyte interface (SEI) and Z_{CEI} the impedance of the cathode electrolyte interface (CEI). Stripping describes the re-intercalation of metallically deposited lithium. Research has shown that the stripping reaction leads to a plateau in the voltage relaxation profile (VRP) [15, 16] and therefore, can be used as an additional indicator for lithium plating during the charging process.
The parallel impedance introduced by the plating reaction leads to an abnormal decrease in the overall cell impedance during the charging process [13, 17]. This results in a change in curvature, which could serve as an input parameter for impedance-based control of the charging current. The experimental setup introduced in subsection 2.2 is capable of a target current specification for the battery cycler. This allows the development of a real-time impedance-based charging algorithm where lithium-plating is reliably detected while operating the LIB at its electrical and thermal limits to minimize the charging time. To enable such control, the onset of the lithium plating reaction has to be reliably detected.

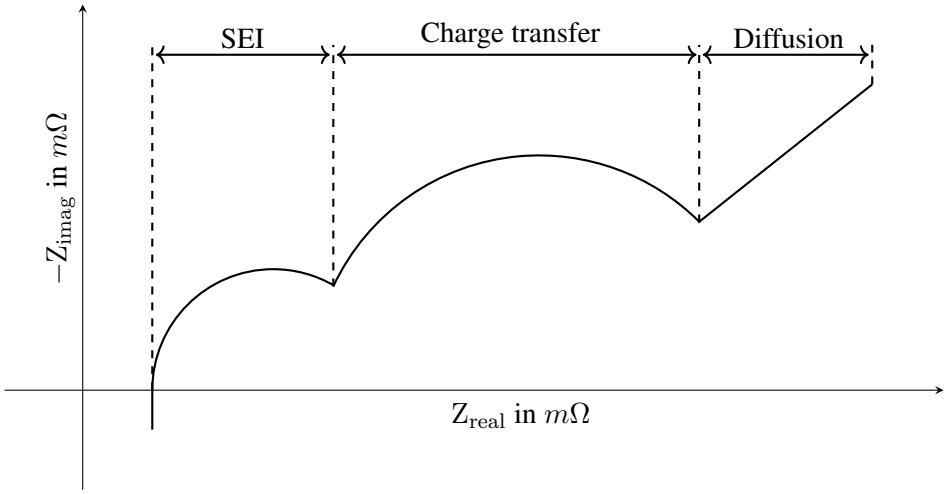

Figure 1: Impedance spectrum visualized in a Nyquist plot with the different sections related to the corresponding kinetic process

2 Experimental procedure

Previous studies have analyzed the influence of various charging rates [13, 17–20] and temperatures [13, 17–20] on the impedance. Koleti et al. [19] used a current interruption technique with a pause of 3 s every $1\,\%$ SOC to track the impedance ZTR at the transition frequency f_{tr} at which the impedance changes to a $45°$ slope. The authors were able to detect lithium plating with current rates of up to $1.25\,\mathrm{C}$. However, an interruption of the charging current contradicts the goal of a minimal charging time. Koseoglou et al. [13] utilized DEIS to successfully detect the onset of lithium plating in high-energy and high-power cells during charging processes with up to 6 C using a single-sine sweep excitation. The used frequency ranges of $3.2\,\mathrm{kHz}$ to $0.2\,\mathrm{Hz}$ and $3.2\,\mathrm{kHz}$ to $1\,\mathrm{Hz}$ lead to a measurement time of $32.35\,\mathrm{s}$ and $9.19\,\mathrm{s}$, respectively, which corresponds to a SOC variation of $1.5\,\%$ during the measurement of one impedance spectrum in the worst case scenario. For the post-processing of the data, Shen et al. [17] used a Savitzky-Golay filter with no further specification on the parameters used for smoothing. The extreme conditions during

fast-charging lead to a complex coupling of electrical and thermal effects which represents an additional challenge besides applying EIS on a non-linear system. As temperature increases during charging, the cell impedance decreases [17], while higher SOCs increase the likelihood of lithium plating [6]. When charging from a higher initial SOC, the cell exhibits a less pronounced self-heating effect upon reaching the target SOC, compared to a charging process starting from a lower SOC. Due to the higher impedance, the plating reaction is expected to initiate earlier during the charging procedure. Moreover, lower ambient temperatures result in higher initial impedance and thus in stronger self-heating, compared to higher temperatures. This, in turn, could also affect the onset of lithium plating. To ensure reliable detection of lithium plating during fast charging, it is crucial to consider these interrelated effects. To decouple the different effects, a systematic investigation under various operating conditions is necessary while addressing potential disturbing factors which could hinder the reliable detection of lithium plating. So far, the effect of the initial SOC at the beginning of the charging process remains largely unexplored. To address the existing research gap and to examine the influence of metallic lithium deposition on battery impedance, a series of experiments at different starting SOCs, charging currents, and ambient temperatures were conducted.

2.1 Lithium-ion cell under investigation

Two commercially available lithium-ion 18650 cells have been used to investigate the influence of lithium plating on the cell impedance. The TerraE-INR18650-25P (TerraE) is a high-power cell with a nickel-rich NCA cathode and a graphite anode with silicon added. The properties and characteristics of the cell are presented in Table 1.

Table 1: Properties of the cell under investigation

Manufacturer	TerraE
Model	INR18650-25P
Maximum Voltage	4.2 V
Minimum Voltage	2.5 V
Nominal Capacity	2.5 Ah
Standard Charging Rate	0.5 C

Before the dynamic impedance measurements, an initial electrochemical characterization was carried out, including a capacity measurement with a C/3 constant current constant voltage (CC-CV) discharge, using a cut-off current of C/10 to determine the initial capacity C_0. For the internal resistance R_0, an EIS measurement at $50\,\%$ SOC was conducted. The internal resistance was calculated through linear interpolation to obtain the real part at the zero crossing of the y-axis. Table 2 gives an overview over the measured capacities and internal resistances for each cell used in the experiments.

Table 2: Initial capacity C_0 and initial internal resistance R_0 of the cells under investigation

Cell No.	**TerraE_1**	**TerraE_2**
Capacity C_0	2515.80 mAh	2511.18 mAh
Internal resistance R_0	14.68 mΩ	14.83 mΩ

2.2 Experimental setup

To realize the DEIS measurements, an Inspectrum.10-5 ES impedance measurement device of the manufacturer Safion (Aachen, Germany) is used in combination with an XCTS40A battery cycler of the manufacturer BaSyTec (Asselfingen, Germany). Both devices are connected simultaneously to the battery during the experiment. Inspectrum.10-5 ES provides the AC excitation while the XCTS40A is used for the DC current, resulting in an impedance measurement under dynamic conditions. To extend the experimental setup, an Inspectrum.MUX by Safion is connected to the Inspectrum.10-5 ES, which allows the investigation of up to 8 cells. Note that the AC excitation is only multiplexed across the different channels, which means only one cell can be measured at a time. The schematic setup is shown in Figure 2. Both devices have a CAN interface, which enables real-time communication and the exchange of variables and data. To control the devices during the charging process, a python framework was developed and implemented onto RaspberryPi microcontrollers.
For the execution, a master is required that acts as a scheduler, in case, two measurements are initiated simultaneously. The master receives a starting command from the battery cycler at the beginning of the charging process. The corresponding channel is then added to a queue and a CAN message is sent to the Inspectrum.10-5 ES in defined intervals, to initiate the dynamic impedance measurement. When the

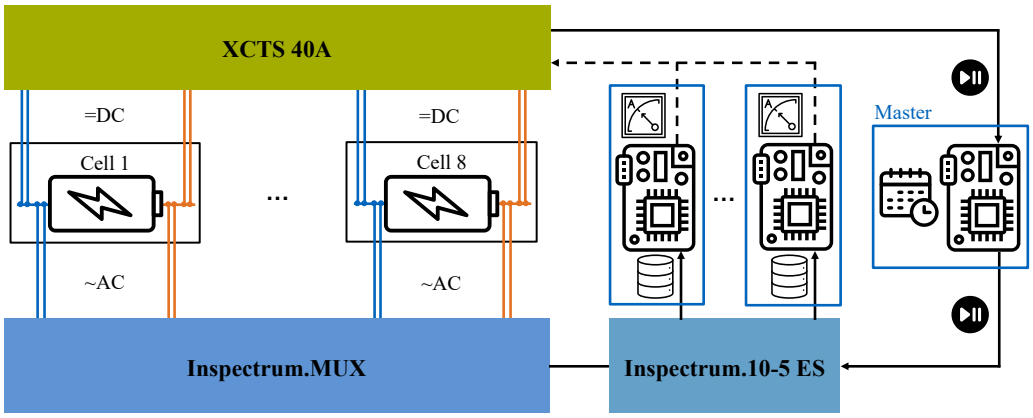

Figure 2: Schematic drawing of the experimental setup used for the dynamic electrochemical impedance spectroscopy investigations.

DEIS is finished, the data is transferred via the CAN bus to an individual RaspberryPi for the corresponding channel to process the data. This setup can also be used to generate a target current specification for the battery cycler indicated by the dashed lines in Figure 2. Note that the simultaneous connection of both measurement devices to the battery results in a parallel connection between the LIB and the battery cycler.

2.3 Methodology

For the experiments, a frequency range from 2 kHz to 5 Hz with 32 frequencies and an peak-to-peak excitation current of 400 mA was used in combination with a non-linear drift correction. For the experiments, 3 measures per frequency were chosen, resulting in a excitation time of about 0.6 s. In combination with the required time to connect to a channel and the time needed to send the data on the CAN bus, this leads to an overall cycle time of about 2 s per measurement. To record the voltage relaxation, a pause of 30 min was added after the charging processes and the battery voltage was recorded in increments of 500 ms. For precharging and discharging the cells, a CC-CV procedure has been chosen with a C-rate of C/3 and C/10 as a cut-off criterion. The cells were investigated at 25 °C and 10 °C using a IPP110eco climate chamber by Memmert (Germany). Table 3 gives an overview over the different test cases for each individual cell. The chosen set of parameters is based on the hypothesis that test cases involving high stress factors will result in a detectable amount of lithium plating, whereas conditions with lower current rates and higher ambient temperatures are not expected to trigger lithium plating.

Table 3: Experimental test cases

Cell	TerraE_1	TerraE_2
Temperature	10 °C	25 °C
Start SOC	10 % to 40 % 10 % steps	10 % to 40 % 10 % steps
End SOC	80 %	95 %
C-rate	1 C to 4 C 1 C steps	1 C to 4 C 1 C steps

3 Results

For the execution of the DEIS during the charging process, a C-rate-based interval was used, so one measurement of every 0.5 % SOC was derived. According to Koseoglou et al. [13] the imaginary part has advantages for the detection of lithium plating compared to the real part because of its lower dependency on SOC, temperature, and relaxation time. For the evaluation of the impedance data, the imaginary part at 15 Hz was selected as a compromise between signal-to-noise-ratio (SNR) and emphasizing low frequencies. In the following, the Nyquist plots and the voltage relaxation profiles (VRPs) for the experimental test cases are presented. For the postprocessing of the impedance data, a Savitzky-Golay filter

was used with a 3rd order polynomial and a window size of 75 % of the data. For the analysis of the VRP, a moving-average filter was used with a window size equal to 5 % of the data.

3.1 Experiments at 10 °C

Figure 3 shows the results of the VRP for TerraE_1. According to the literature, lithium plating can be detected through plateaus in the relaxation profile. In this case, no evidence of metallic deposition of lithium can be identified. One has to note that the VRP method is insensitive to small amounts of lithium plating [21], which could possibly hinder the successful detection. For charging rates of 1 C and 2 C, the VRPs in Figure 3 (a) and Figure 3 (b) show no visible influence of the initial SOC on the voltage relaxation. When it comes to higher currents of 3 C and 4 C, a slight shift to the right with increasing starting SOC can be observed. The shift is more pronounced for the 4 C charging procedure. The results of the DEIS experiments at 10 °C temperature are presented in Figure 4. The impedance shows a strong decrease in the beginning of the charging process, related to the self-heating of the cell. After the initial decrease, the impedance remains mostly constant. For higher charging rates and lower initial SOCs, this effect is more pronounced. In the case of charging with 1 C, no abnormal drop in the impedance can be detected, while for the charging processes with 2 C and initial SOCs of 10 % to 30 % a change in curvature at 70 % SOC can be detected. In theory, this drop could indicate the onset of lithium plating. As the drop occurs at the same time and at the end of the charging process for the initial SOCs of 10 % to 30 %, and the VRP (Figure 3 (b)) shows no indications of lithium metal deposition, the drop is attributed to the smoothing parameters chosen for this experiments, as this could lead to false positive detection of lithium plating. This phenomenon will be further addressed in section 4. For even higher charging rates of 3 C and 4 C, only the impedance of the 3 C charge with an initial SOC of 30 % shows another deflection of the impedance curve. This could be attributed to an unsuitable parameter set for the post-processing of the data or to the onset of lithium metal deposition.

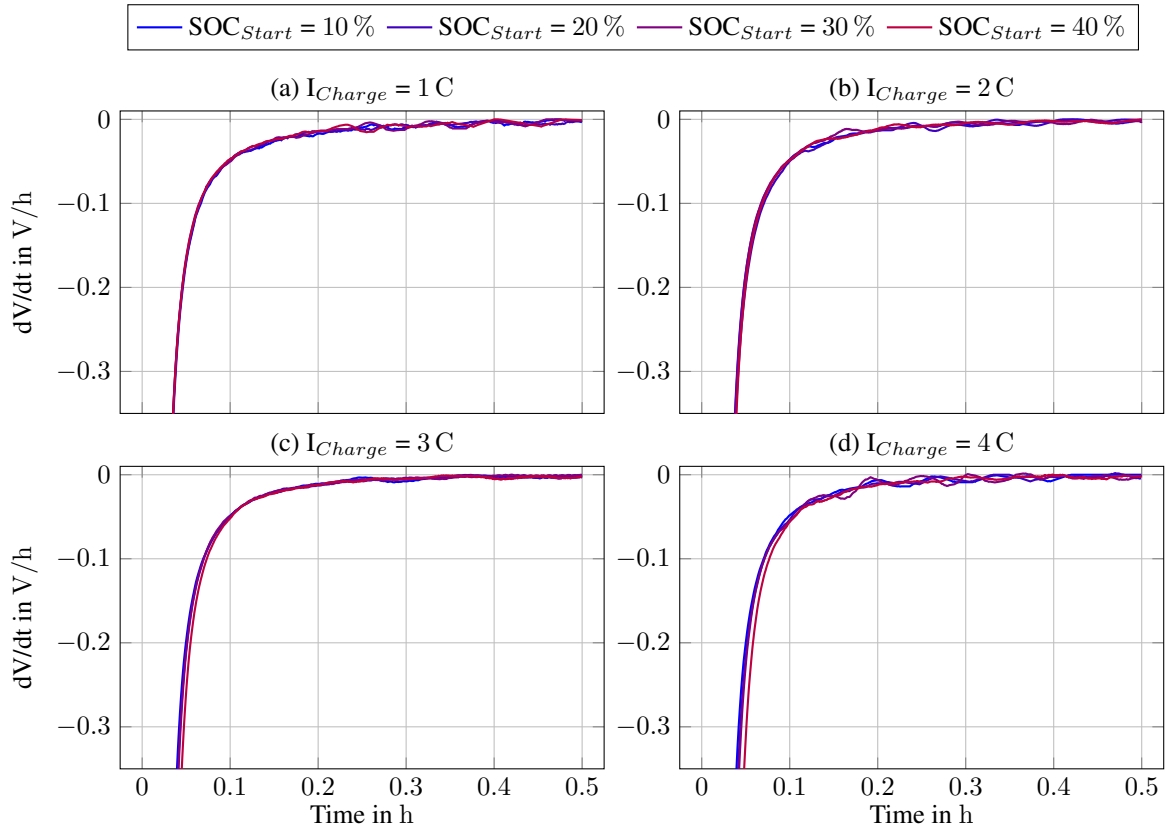

Figure 3: Voltage relaxation profile results for the investigated TerraE_1 cell at 10 °C ambient temperature with different initial SOCs and charging rates.

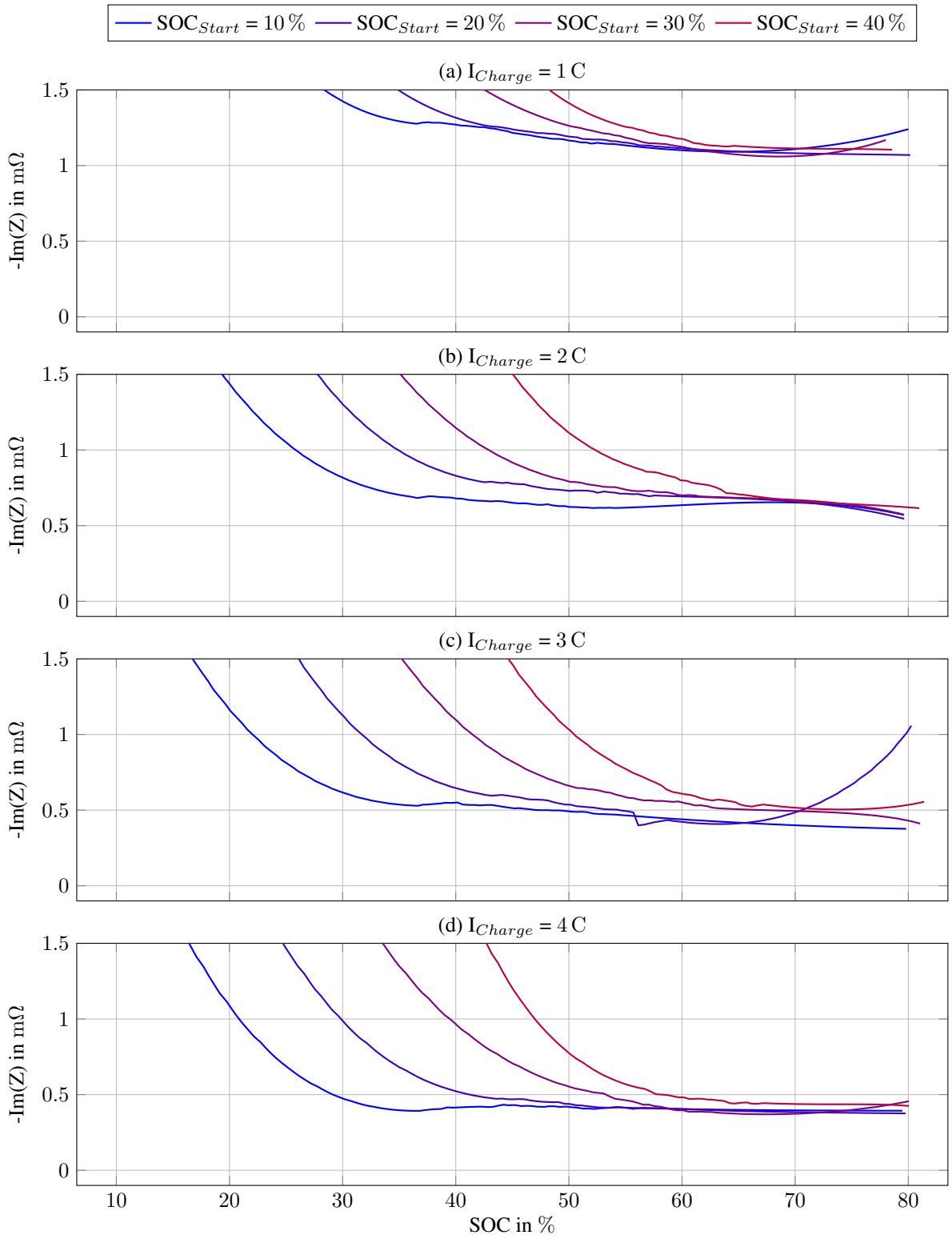

Figure 4: Dynamic electrochemical impedance spectroscopy results for the investigated TerraE_1 cell at 10 °C ambient temperature with different initial SOCs and charging rates.

3.2 Experiments at 25 °C

The VRPs for the experiments at 25 °C (Figure 5) show normal relaxation behaviour with no further indication for lithium plating during the charging process. Despite the same smoothing method, the VRPs show more noise in the area from 0.1 h to 0.5 h. As the experiments were conducted on different

channels of the XCTS40A, this could be a channel related effect. Compared to the experiments conducted at 10 °C, the VRPs show no shift to the right with higher initial SOCs. Therefore, it can be concluded, that no influence of the initial SOC on the probability of lithium plating can be observed under this conditions. The results for the DEIS experiments on the TerraE_2 cell are presented in Figure 6. The imaginary part shows a strong initial decrease, related to the self-heating process inside the cell. After the initial drop, a phase with almost constant impedance values can be observed for initial SOCs of 10 % and 20 %. The imaginary part for initial SOCs of 30 % and 40 % follows a U shape with only very short phases of constant impedance, compared to the bathtub shape reported in literature [13]. All of the experiments show a strong impedance increase at the end of the charging process, starting at about 80 % SOC, which can be attributed to the CV-phase. The reduced charging current during the CV-phase leads to an increased impedance of the XCTS40A battery cycler, and consequently, a higher overall impedance of the parallel connection. Again no clear deflection of the impedance curves can be observed in the investigated test cases. The impedance of the charge transfer is mostly influenced by the SOC and the temperature. For an identical SOC, the difference in the impedance can be attributed to the temperature when considering charging procedures with the same C-rate. When comparing the impedance values for the different initial SOCs at a certain state of charge, e.g., 50 %, it can be seen that higher starting SOCs lead to a higher value of the imaginary part of the impedance, which can be attributed to a reduced temperature at this specific SOC. Therefore, the probability of lithium plating under these circumstances should be higher compared to charging processes, which started at lower SOCs. It can also be observed, that the difference in the imaginary part becomes smaller when reaching higher SOCs. The experiments for a charging rate of 1 C had to be repeated due to issues in the data acquisition. The impedance for initial SOCs of 20 % to 40 % shows lower values compared to higher charging rates, despite lower temperatures and a higher impedance influence of the battery cycler. In addition, the impedance does not follow the typical bathtub shape reported in literature.

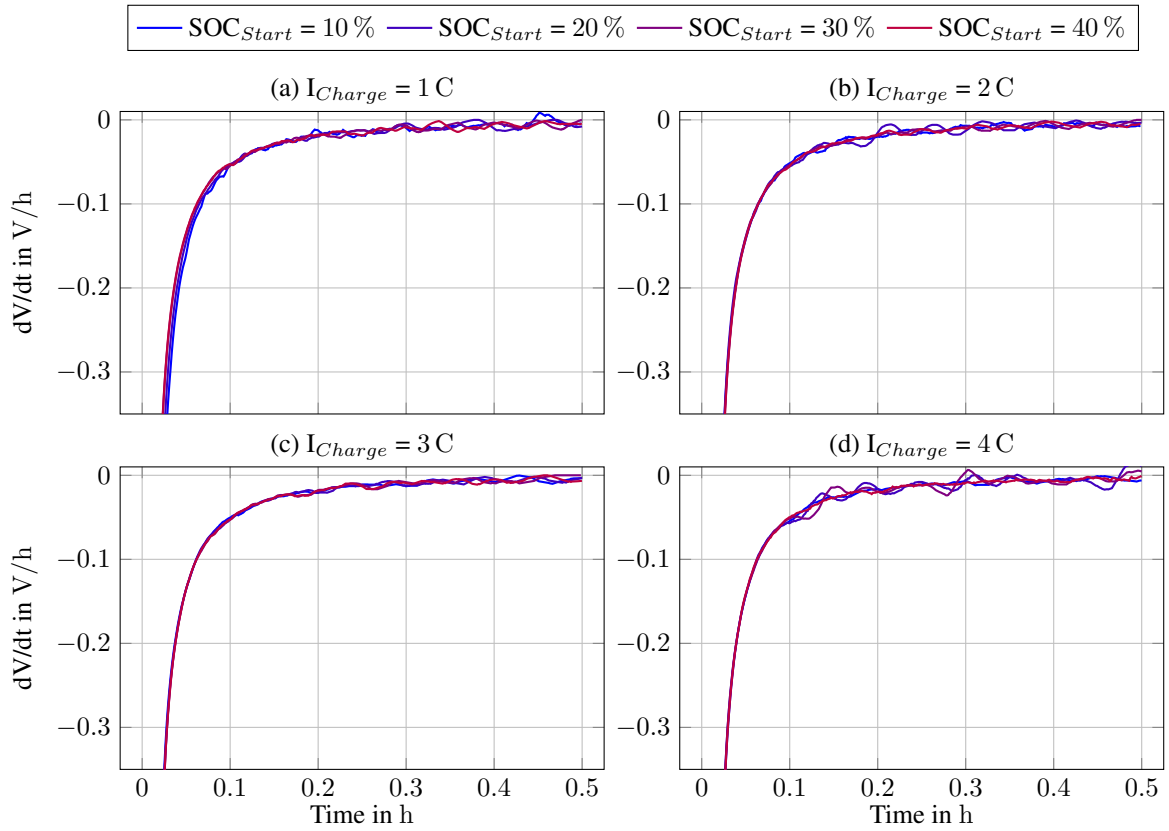

Figure 5: Voltage relaxation profile results for the investigated TerraE_2 cell at 25 °C ambient temperature with different initial SOCs and charging rates.

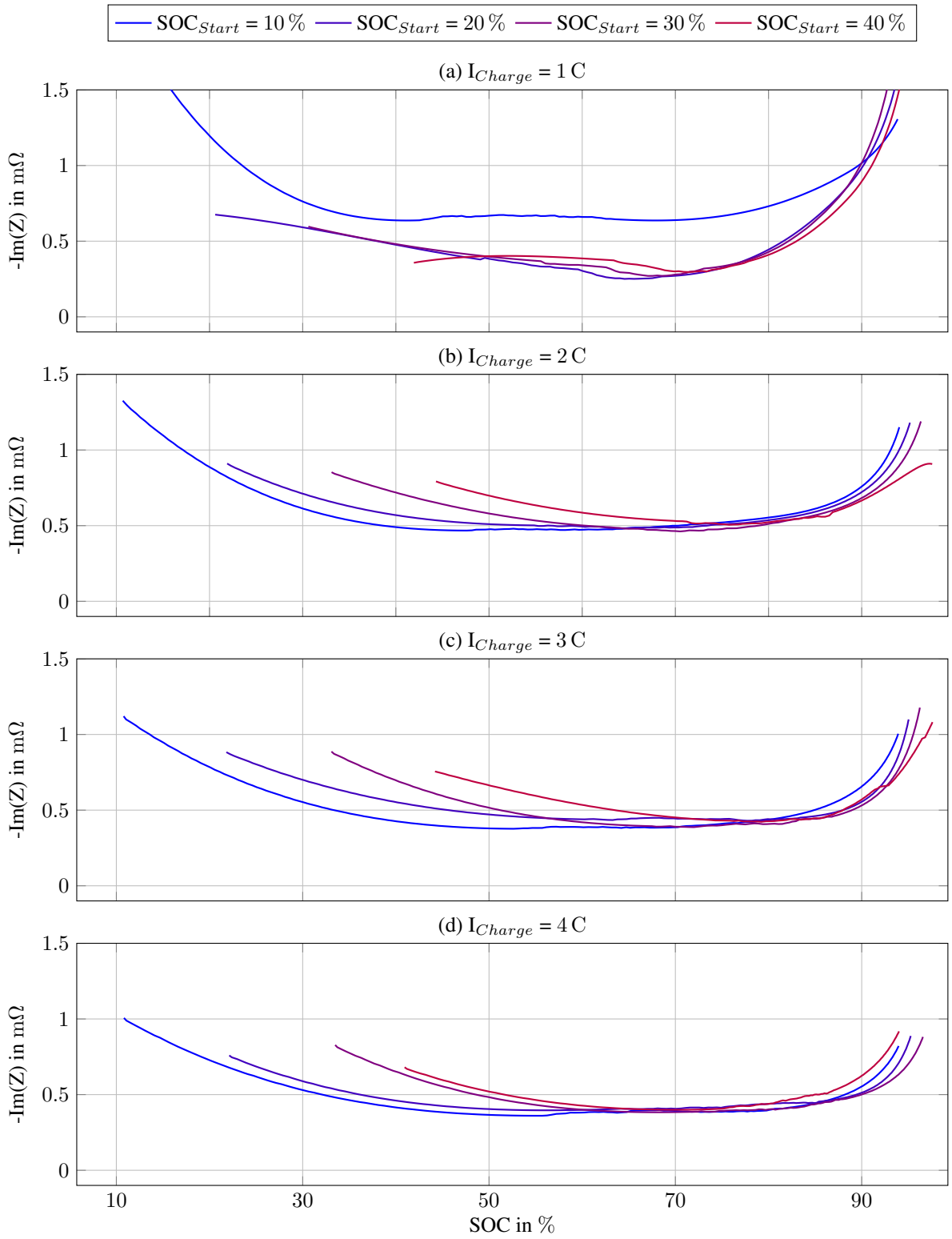

Figure 6: Dynamic electrochemical impedance spectroscopy results for the investigated TerraE_2 cell at 25 °C ambient temperature with different initial SOCs and charging rates.

4 Discussion

The results presented in the previous chapter show no indications of metallic lithium deposition on the anode surface, despite considering high charging rates, variations in the initial SOC and different temper-

atures. These findings contradict both the initial hypothesis of this study and the observations reported in the literature [13]. There are two possible explanations for the observed behaviour of the cell:

(i) The used parameter set in this study is not able to trigger the metallic lithium deposition. This is supported by the derived VRP profiles. In the study of Koseoglou et al. [13], the VRP for charging processes without lithium plating showed a shift to the right with increased C-rate. For even higher currents, lithium plating could be detected through a two stage plateau in the VRP. In the conducted experiments of this study, a similar shift to the right could be observed for the experiments with $3\,\mathrm{C}$ and $4\,\mathrm{C}$ at $10\,^{\circ}\mathrm{C}$ for increased initial SOCs, which indicates that the stress factors were not high enough to trigger the lithium deposition. This would lead to the assumption, that the TerraE cell is capable of a $15\,\mathrm{min}$ fast-charge at $10\,^{\circ}\mathrm{C}$ when in a new and fully equilibrated condition with no or only low inhomogeneities inside the cell, despite the fact that the applied charging rate considerably exceed the manufacturer's recommended fast-charging rate of $1.6\,\mathrm{C}$ at $25\,^{\circ}\mathrm{C}$. High surface film resistances can also induce lithium plating [22] and, in addition, an inhomogeneous SEI resistance can lead to local current peaks [23], which increase the probability of lithium plating. When assuming a homogeneous SEI with a low resistance for a new cell, this would further support the non-occurrence of plating.

(ii) The applied diagnostic methods - DEIS and VRP - failed to detect the metallic deposition. According to Schmidt et al. [24], the SNR during the DEIS measurement is decreased and therefore, also the quality of the derived impedance data. In addition, multi-sine excitation has negative effects on the measurement quality [10]. This could lead to the possibility that the derived data quality was too low to detect the abnormal impedance drop, despite that the galvanostatic peak-to-peak excitation of $400\,\mathrm{mA}$ resulted in a voltage response of about $5\,\mathrm{mV}$, which is in line with literature recommendations [25]. For future experiments it may be beneficial to use less frequency points and a higher current excitation for a better voltage response to improve data quality. In addition, it needs to be investigated why the experiments conducted at $25\,^{\circ}\mathrm{C}$ with a $1\,\mathrm{C}$ charge showed abnormal behaviour. The TerraE cell uses an anode with a mixture of graphite and silicon, while the experiments in the literature were conducted on pure graphite anodes [13, 18, 19]. With silicon another possible influencing factor is introduced and further investigations are necessary to understand, how the behaviour of the impedance and voltage relaxation is affected in case of a plating event. In addition, the voltage relaxation is used to observe the stripping reaction. If the deposited lithium is fully irreversible, no stripping is occurring and the VRP method fails to detect it.

To prove these findings, further experiments are necessary which will be presented in section 5. After the data has been collected, the next step is the filtering and smoothing of the data. Shen et al. [17] also used a Savitzky-Golay filter for the post-processing of their data. As shown in Figure 7, a trade-off between the smoothness of the data and the accurate representation of the raw data has to be made when applying a filtering method. Using a window size of $100\,\%$ would lead to a false detection of lithium plating at the end of the charging process. Similar behaviour can be observed when applying the Savitzky-Golay filter on the VRP (Figure 8). Using a window with the size of $10\,\%$ of the data length, a deflection in the curve can be observed which could also lead to a false detection of lithium plating during the charging process. For additional information on plating detection via DEIS or VRP, the reader is referred to [13] and [26].

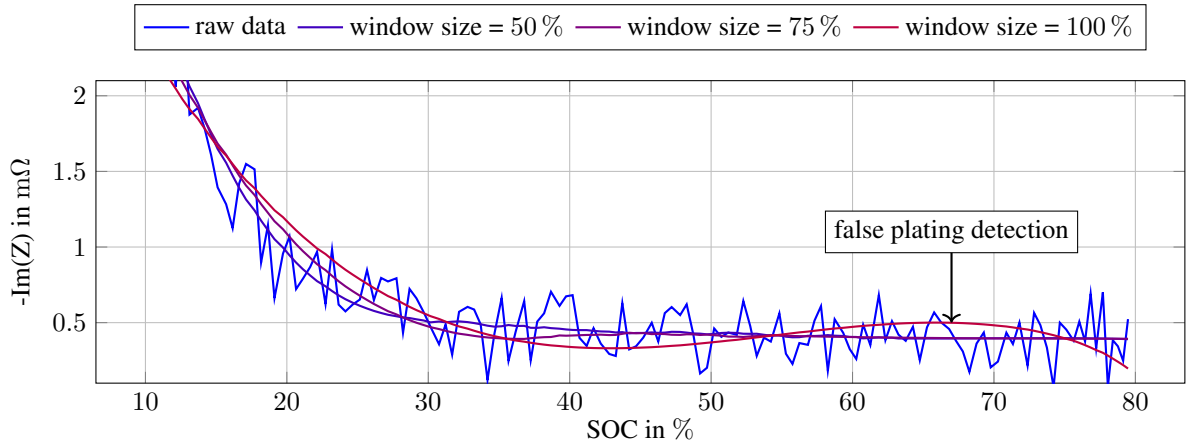

Figure 7: Influence of different smoothing parameters in the Savitzky-Golay filter on the impedance data exemplarily shown for the experiment at $10\,^{\circ}\mathrm{C}$ with a initial SOC of $10\,\%$ and a charging rate of $4\,\mathrm{C}$.

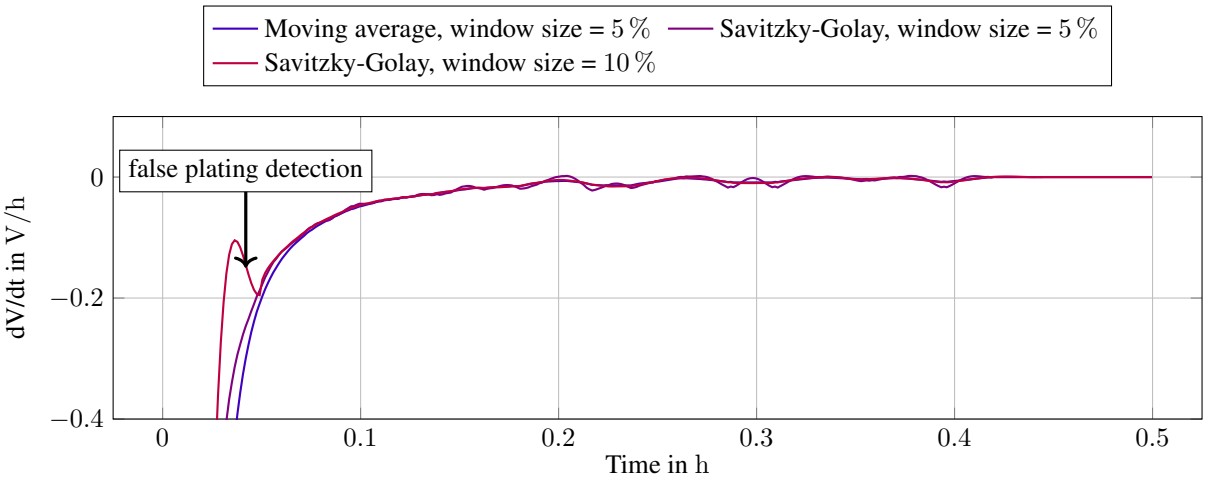

Figure 8: Influence of different smoothing parameters in the Savitzky-Golay filter on the VRP exemplarily shown for the experiment at 10 °C with a initial SOC of 10 % and a charging rate of 4 C.

5 Conclusion and Outlook

In this study, a series of DEIS experiments under different charging rates, initial SOCs and temperatures were conducted. The analysis of the impedance data and the VRP did not show any indications for lithium metal deposition, which contradicts the original hypothesis of this paper and the observations reported in the literature. It could be shown that the parameters used for the post-processing of the data have a major influence on the conclusion that can be drawn from such experiments. When using dynamic impedance measurements for the detection of lithium plating, high data quality is also of utmost importance. One of the main challenges in reliably detecting the onset of the metallic deposition lies in ensuring good quality of the DEIS data, especially when using multi-sine excitation in combination with suitable filtering parameters to prevent false positive detections of lithium plating. In addition, further investigations are necessary to fundamentally understand how the silicon content in the anode influences the robustness of the methodologies proposed in the literature. To validate or falsify the initial hypothesis of this paper, a follow-up experimental series will be carried out with the test cases described in Table 4. The reduced ambient temperature in combination with the increased maximum C-rate is expected to promote the metallic lithium deposition. A second test case is designed to induce inhomogeneities and ageing effects, which should lead to local current peaks and inhomogeneous SEI resistance and thereby increasing the likelihood of lithium plating. In addition, a post-mortem analysis will be conducted to verify the conclusions drawn from the results. In summary, these findings underscore the inherent complexity in accurately detecting lithium plating under dynamic conditions. Nevertheless, the forthcoming experimental series is expected to make a valuable contribution to improving detection protocols and advancing the broader understanding of electrochemical deposition phenomena.

Table 4: Future experimental test cases

Test case no.	**1**	**2**
Temperature	0 °C	0 °C
Start SOC	0 % to 40 % 10 % steps	0 %
End SOC	100 %	100 %
C-rate	1 C to 6 C 1 C steps	4 C
Number of cycles per parameter set	1	100

References

[1] A. Jossen and W. Weydanz, *Moderne Akkumulatoren richtig einsetzen*, 2nd ed. Göttingen: MatrixMedia Verlag, 2019.

[2] A. Tomaszewska, Z. Chu, X. Feng, S. O'Kane, X. Liu, J. Chen, C. Ji, E. Endler, R. Li, L. Liu, Y. Li, S. Zheng, S. Vetterlein, M. Gao, J. Du, M. Parkes, M. Ouyang, M. Marinescu, G. Offer, and B. Wu, "Lithium-ion battery fast charging: A review," *eTransportation*, vol. 1, 2019.

[3] D. Howell, S. Boyd, B. Cunningham, S. Gillard, and L. Slezak, "Enabling fast charging: A technology gap assessment."

[4] F. Katzer and M. A. Danzer, "Analysis and detection of lithium deposition after fast charging of lithium-ion batteries by investigating the impedance relaxation," *Journal of Power Sources*, vol. 503, 2021.

[5] M.-T. F. Rodrigues, K. Kalaga, S. E. Trask, D. W. Dees, I. A. Shkrob, and D. P. Abraham, "Fast charging of li-ion cells: Part i. using li/cu reference electrodes to probe individual electrode potentials," *Journal of The Electrochemical Society*, vol. 166, no. 6, pp. 996–1003, 2019.

[6] N. Wassiliadis, J. Kriegler, K. A. Gamra, and M. Lienkamp, "Model-based health-aware fast charging to mitigate the risk of lithium plating and prolong the cycle life of lithium-ion batteries in electric vehicles," *Journal of Power Sources*, vol. 561, 2023.

[7] T. Waldmann, B.-I. Hogg, M. Kasper, S. Grolleau, C. G. Couceiro, K. Trad, B. P. Matadi, and M. Wohlfahrt-Mehrens, "Interplay of operational parameters on lithium deposition in lithium-ion cells: Systematic measurements with reconstructed 3-electrode pouch full cells," *Journal of The Electrochemical Society*, vol. 163, no. 7, pp. 1232–1238, 2016.

[8] M. Petzl and M. A. Danzer, "Nondestructive detection, characterization, and quantification of lithium plating in commercial lithium-ion batteries," *Journal of Power Sources*, vol. 254, pp. 80–87, 2014.

[9] M. Petzl, M. Kasper, and M. A. Danzer, "Lithium plating in a commercial lithium-ion battery – a low-temperature aging study," *Journal of Power Sources*, vol. 275, pp. 799–807, 2015.

[10] S. Gantenbein, M. Weiss, and E. Ivers-Tiffée, "Impedance based time-domain modeling of lithium-ion batteries: Part i," *Journal of Power Sources*, vol. 379, pp. 317–327, 2018.

[11] K. Mc Carthy, H. Gullapalli, K. M. Ryan, and T. Kennedy, "Review—use of impedance spectroscopy for the estimation of li-ion battery state of charge, state of health and internal temperature," *Journal of The Electrochemical Society*, vol. 168, no. 8, 2021.

[12] C. Uhlmann, J. Illig, M. Ender, R. Schuster, and E. Ivers-Tiffée, "In situ detection of lithium metal plating on graphite in experimental cells," *Journal of Power Sources*, vol. 279, pp. 428–438, 2015.

[13] M. Koseoglou, E. Tsioumas, D. Ferentinou, N. Jabbour, D. Papagiannis, and C. Mademlis, "Lithium plating detection using dynamic electrochemical impedance spectroscopy in lithium-ion batteries," *Journal of Power Sources*, vol. 512, 2021.

[14] Y. Liu, L. Wang, D. Li, and K. Wang, "State-of-health estimation of lithium-ion batteries based on electrochemical impedance spectroscopy: a review," *Protection and Control of Modern Power Systems*, vol. 8, no. 1, 2023.

[15] X.-G. Yang, S. Ge, T. Liu, Y. Leng, and C.-Y. Wang, "A look into the voltage plateau signal for detection and quantification of lithium plating in lithium-ion cells," *Journal of Power Sources*, vol. 395, pp. 251–261, 2018.

[16] D. Ren, K. Smith, D. Guo, X. Han, X. Feng, L. Lu, M. Ouyang, and J. Li, "Investigation of lithium plating-stripping process in li-ion batteries at low temperature using an electrochemical model," *Journal of The Electrochemical Society*, vol. 165, no. 10, pp. A2167–A2178, 2018.

[17] Y. Shen, X. Wang, Z. Jiang, B. Luo, D. Chen, X. Wei, and H. Dai, "Online detection of lithium plating onset during constant and multistage constant current fast charging for lithium-ion batteries," *Applied Energy*, vol. 370, 2024.

[18] T. Sun, Z. Li, G. Zhu, L. Wang, D. Ren, T. Shen, L. Lu, Y. Zheng, X. Han, and M. Ouyang, "Impedance-based online detection of lithium plating for lithium-ion batteries: Mechanism and sensitivity analysis," *Electrochimica Acta*, vol. 496, 2024.

[19] U. R. Koleti, T. Q. Dinh, and J. Marco, "A new on-line method for lithium plating detection in lithium-ion batteries," *Journal of Power Sources*, vol. 451, p. 227798, 2020.

[20] X. Wang, J. Li, S. Chen, G. Zhang, B. Jiang, X. Wei, and H. Dai, "Online detection of lithium plating onset for lithium-ion batteries based on impedance changing trend identification during charging processes," *IEEE Transactions on Transportation Electrification*, vol. 9, no. 2, pp. 3487–3497, 2022.

[21] I. D. Campbell, M. Marzook, M. Marinescu, and G. J. Offer, "How observable is lithium plating? differential voltage analysis to identify and quantify lithium plating following fast charging of cold lithium-ion batteries," *Journal of The Electrochemical Society*, vol. 166, no. 4, pp. A725–A739, 2019.

[22] A. N. Jansen, D. W. Dees, D. P. Abraham, K. Amine, and G. L. Henriksen, "Low-temperature study of lithium-ion cells using a liysn micro-reference electrode," *Journal of Power Sources*, vol. 174, no. 2, pp. 373–379, 2007.

[23] M. Ecker, P. Shafiei Sabet, and D. U. Sauer, "Influence of operational condition on lithium plating for commercial lithium-ion batteries – electrochemical experiments and post-mortem-analysis," *Applied Energy*, vol. 206, pp. 934–946, 2017.

[24] J. P. Schmidt, S. Arnold, A. Loges, D. Werner, T. Wetzel, and E. Ivers-Tiffée, "Measurement of the internal cell temperature via impedance: Evaluation and application of a new method," *Journal of Power Sources*, vol. 243, pp. 110–117, 2013.

[25] E. Barsoukov and J. R. Macdonald, Eds., *Impedance Spectroscopy: Theory, Experiment, and Applications*, 2nd ed. John Wiley & Sons, Inc., 2018.

[26] S. Schindler, M. Bauer, M. Petzl, and M. A. Danzer, "Voltage relaxation and impedance spectroscopy as in-operando methods for the detection of lithium plating on graphitic anodes in commercial lithium-ion cells," *Journal of Power Sources*, vol. 304, pp. 170–180, 2016.

Presenter Biography

Raphael Urban received his bachelor's degree in mechanical engineering and his master's degree in automotive engineering from the Technical University of Munich (TUM) in 2020 and 2023. He is currently pursuing a Ph.D. degree with the Institute of Automotive Technology at TUM. His research is focused on dynamic electrochemical impedance spectroscopy for fast-charging of lithium-ion batteries.